Articles

Following the Rotational Trajectory of the Principal Hydrodynamic Frame of a Protein Using Multiple Probes†

Thomas P. Burghardt* and Katalin Ajtai

Department of Biochemistry and Molecular Biology, Mayo Foundation, Rochester, Minnesota 55905

Received November 24, 1993; Revised Manuscript Received February 16, 1994®

ABSTRACT: A generalized set of fluorescence polarization intensities and electron paramagnetic resonance (EPR) spectra from multiple fluorescent and EPR probes of a specific site on an oriented and immobilized protein element in a biological assembly, combined with anisotropic rotational relaxation studies of the purified and labeled protein element freely rotationally diffusing in solution, are used to determine the angular distribution of the principal hydrodynamic frame of the protein element in the biological assembly. This multiprobe analysis method removes all of the basic ambiguities in the measured principal frame angular distribution introduced by limitations or symmetries intrinsic to standard fluorescence polarization intensity ratios and EPR spectra. The angular distribution of the principal frame is also more highly resolved than that previously reported for multiprobe determinations of probe angular distributions and is more useful for determining biological mechanisms because it indicates the order and orientation of the protein element rather than that of the extrinsic probe. Application of this method to the determination of the principal hydrodynamic frame distribution of myosin cross-bridges in muscle fibers in four physiological states, including the active isometric state, demonstrates the method's practicality by indicating the path of cross-bridge orientation changes during the active cycle [Ajtai, Toft, & Burghardt (1994) *Biochemistry* (following paper in this issue)].

The molecular mechanism for force development in muscle involves the proteins myosin and actin and apparently the rotation of the myosin head (cross-bridge) relative to the actin filament. In the past we showed that signals from luminescent and paramagnetic probes attached to the cross-bridge report information about their orientation that we combined to form a relatively complete picture of cross-bridge rotation upon nucleotide binding (Burghardt & Ajtai, 1992; Ajtai et al., 1992). This previous work using multiple extrinsic probes indicated the probe orientation distributions in two physiological states of the fiber and confirmed earlier observations of cross-bridge rotation upon nucleotide binding or activation (Borejdo et al., 1982; Burghardt et al., 1983; Ajtai & Burghardt, 1986). We report here on the development of new methods to indicate a highly resolved angular distribution of the principal hydrodynamic reference frame of cross-bridges in fibers. We measure the principal axis distribution of cross-bridges in four physiological states of the fiber, including the active isometric state. This description indicates the pathway of cross-bridge rotation during contraction, providing new insight into the molecular mechanism of muscle contraction.

The principal hydrodynamic frame of a protein is an appropriate reference for describing both the rotational movement of the protein relative to the laboratory frame and the orientation of an extrinsic probe attached to the protein. For protein motion, the principal frame indicates the rotation of readily identifiable features of the protein (for instance, rotation about the long or short axis of an ellipsoid of revolution that approximates the shape of the myosin head). This feature, applied to cross-bridge motion during contraction, will resolve the longstanding ambiguity in the interpretation of probe data related to whether or not the myosin cross-bridge power stroke invokes a polar, a torsional, or both kinds of angular change in the cross-bridge orientation. Likewise, when extrinsic probes were used without reference to the principal frame, the observation of differential sensitivity to cross-bridge rotation by various probes of the cross-bridge led some to believe that the probe data were inconsistent (Burghardt & Ajtai, 1990). However, by relating all probe orientations to the principal frame of the cross-bridge, we will be able to account for the differential sensitivity of probes as consistent with protein rotation.

We showed that the multiple probe study of the orientation of proteins in ordered assemblies enhances the resolution of the detectable probe angular distribution over that available from a single probe study (Burghardt & Ajtai, 1992; Ajtai et al., 1992). The resolution enhancement results from (i) the combination of complementary data from different signal donors, i.e., that electron paramagnetic resonance (EPR) spectral data combine with fluorescence polarization (FP) intensity data, and (ii) the combination of data from similar signal donors that are variously oriented on the protein of interest. However, some basic ambiguities remained in the probe distribution that were impossible to remove with the old formalism. The present work demonstrates how to remove these ambiguities using certain FP intensities that sense asymmetries of the probe angular distribution that are not detected by EPR. These FP intensities when combined with the EPR data by the new multiple probe analysis remove all of the fundamental ambiguities in the measured protein angular distribution. Application of the method to the case of cross-bridges in muscle fibers allows us to estimate the path

† This work was supported by grants from the National Institutes of Health (R01 AR 39288), the American Heart Association (Grant-in-Aid 930 06610), and the Mayo Foundation.

* Address correspondence to this author.

® Abstract published in *Advance ACS Abstracts,* April 1, 1994.

0006-2960/94/0433-5376$04.50/0

and extent of cross-bridge rotation during the contraction cycle.

THEORY

(A) The Model-Independent Description of Protein Order. We investigate cross-bridge orientation using direction-reporting extrinsic probes that chemically modify selected side chains on the muscle proteins and fluorescence polarization (FP) or electron paramagnetic resonance (EPR) spectroscopy to detect probe orientation (Nihei et al., 1974; Belágyi, 1975; Thomas & Cooke, 1980). We observe the orientation of the principal hydrodynamic coordinate frame of the protein molecule. A general formalism describes the angular order of the protein in the ordered assembly that is appropriate for either FP or EPR data. The method is model-independent and is based on the expansion of N, the protein angular distribution, in terms of a set of complete angular functions, $D^j_{m,n}$, with unknown coefficients. N is the distribution of the principal protein frame relative to the laboratory frame. Every protein frame is related to the laboratory frame by the Euler rotation angles α, β, and γ, where α and β are the azimuth and polar angles measured relative to the laboratory frame and γ is the torsion angle. We express N as

$$N(\alpha,\beta,\gamma) = \sum_{j=0}^{\infty} \sum_{m,n=-j}^{j} a^j_{m,n}[(2j+1)/8\pi^2]^{1/2} D^j_{m,n}(\alpha,\beta,\gamma) \quad (1)$$

where $a^j_{m,n}$ are the order parameters of rank j that we may observe. FP or EPR detect different subsets of the order parameters (Burghardt, 1984).

The ability of a single extrinsic probe to detect protein rotation depends critically on the probe orientation within the principal frame since a protein rotation that rotates the probe about a symmetry axis (i.e., symmetrical with respect to its signal emission and detection) cannot be detected. We combine data from different probes variously oriented within the principal frame to remove this ambiguity. The muscle fiber system demonstrates the advantage of using multiple probes since cross-bridge rotation is detected by a variety of probes but the sensitivity of any single probe to the changing cross-bridge orientation varies widely.

(B) Mapping Angular Transitions of Proteins Using Multiple Probes. Our description of protein order is flexible enough to be applicable to either FP or EPR data. The EPR spectrum, $E(H)$, and FP intensities, $F(\psi,\chi,\lambda_{ex},\lambda_{em})$, may be interpreted in terms of *probe* order parameters by

$$E(H) = \sum_{i=0}^{i_{max}} a_i g_i^{EPR}(H) \quad (2)$$

and

$$F(\psi,\chi,\lambda_{ex},\lambda_{em}) = \sum_{i=0}^{4} a_i g_i^{FLS}(\psi,\chi,\lambda_{ex},\lambda_{em}) \quad (3)$$

where $g_i^{EPR}(H)$ and $g_i^{FLS}(\psi,\chi,\lambda_{ex},\lambda_{em})$ are basis spectra for EPR and FP experiments, respectively, H is the Zeeman field strength, a_i (representing $a^j_{m,n}$) is a probe order parameter, ψ and χ are angles relating the excitation and emission polarizers to the laboratory frame, and λ_{ex} and λ_{em} are excitation and emission wavelengths (Burghardt & Ajtai, 1992). The limits on the sums over i in eqs 2 and 3 indicate the number of order parameters contributing to the signal.

A coordinate rotation relates the *probe* order parameters to the principal *protein* order parameters in a particular state of the protein such that

$$a^j_{m,n}(probe\ \ell,\ state\ q) = \sum_{k=-j}^{j} a^j_{m,k}(protein,\ state\ q) D^{*j}_{k,n}(\Omega_\ell) \quad (4)$$

where Ω_ℓ are the Euler angles relating the principal protein frame with the ℓth probe frame. The Euler rotation depends only on the index designating the probe. In an ordered sample a similar equation describes the rotational change of state of the labeled protein element such that

$$a^j_{m,n}(protein,\ state\ q) = \sum_{k=-j}^{j} a^j_{m,k}(protein,\ state\ p) D^{*j}_{k,n}(\Omega_{q,p}) \quad (5)$$

where $\Omega_{q,p}$ are the Euler angles relating the principal protein frame in state q with that in state p. Equations 2–5 constrain the protein order parameters and make a set of simultaneous equations solved using a weighted least squares protocol (Strang, 1986). In eqs 2–5 the unknowns are the protein order parameters and the Euler angles Ω.

(C) Estimating the Euler Angles Relating the Protein and Probe Coordinate Frames. (C.1) Steady-State EPR of Spin-Labeled Protein in Solution. The shape of the EPR spectrum of spin-labeled proteins in solution depends on the protein rotational diffusion constants and on the relationship between the principal hydrodynamic and principal magnetic frames of reference. Several previous workers modeled the EPR spectrum of free or restricted rotationally diffusing spin-labeled proteins (McCalley et al., 1972; Goldman et al., 1972; Freed, 1976). We adapted the method and notation of McCalley et al. (1972) for spin-labeled myosin subfragment 1 (S1) assuming that S1 is a prolate ellipsoid. We begin as they did by modifying the Bloch equations for the macroscopic magnetization, **M**, to include rotational diffusion of the spin density in the reference frame rotating at ω, the applied microwave frequency, giving

$$\frac{\partial u}{\partial t} = \frac{-u}{T_2} - \gamma_e(H - H_0)v - \mathcal{L}u \quad (6a)$$

$$\frac{\partial v}{\partial t} = \frac{-v}{T_2} + \gamma_e(H - H_0)u - \gamma_e M_z H_{xy} - \mathcal{L}v \quad (6b)$$

$$\frac{\partial M_z}{\partial t} = -\frac{(M_z - \langle M_z \rangle)}{T_1} + \gamma_e H_{xy} v - \mathcal{L}M_z \quad (6c)$$

where $u = M_x \cos(\omega t) - M_y \sin(\omega t)$, $v = -M_x \sin(\omega t) - M_y \cos(\omega t)$, t is time, T_2 is the spin–spin relaxation time, T_1 is the spin–lattice spin relaxation time, γ_e is the magnetogyric ratio of a bound electron, H is the Zeeman field strength, H_0 is the resonance field strength, H_{xy} is the field strength of the applied microwave field, $\langle M_z \rangle$ is the time-averaged z component of the magnetization, and $\mathcal{L}$ is an operator appropriate for anisotropic rotational diffusion. For an ellipsoid of revolution, $\mathcal{L}$ is given by

$$\mathcal{L} = D_1 L^2 + (D_3 - D_1)L_3 \quad (7)$$

where D_i is the diffusion constant about the ith axis and **L** is the angular momentum operator such that

$$L^2 = \frac{-1}{\sin\beta}\frac{\partial}{\partial\beta}\left(\sin\beta\frac{\partial}{\partial\beta}\right) - \frac{1}{\sin^2\beta}\frac{\partial^2}{\partial\beta^2} \quad (8)$$

$$L_3^2 = \frac{-\partial^2}{\partial\gamma^2} \tag{9}$$

and where β and γ are the polar and torsional degrees of rotational freedom on the domain $0 \le \beta \le \pi$ and $0 \le \gamma \le 2\pi$ as shown in Figure 1 (Davydov, 1963). As done previously, we divide the angular domain of (β, γ) into $N \times M$ discrete zones corresponding to indices n and m such that $\beta_n = (n - {}^1/_2)\Delta_\beta$ and $\gamma_m = (m - {}^1/_2)\Delta_\gamma$, where $\Delta_\beta = \pi/N$ and $\Delta_\gamma = 2\pi/M$ (McCalley et al., 1972). Reexpressing eqs 6–9 in terms of the discrete zones and in the limit where H_{xy} is small, we obtain the two coupled equations

$$0 = -\left(\frac{1}{T_2} + \frac{1}{t_n} + \frac{1}{s_n}\right)u_{n,m} - \gamma_e(H^0_{n,m} - H)v_{n,m} + \Pi(n+1 \to n)u_{n+1,m} + \Pi(n-1 \to n)u_{n-1,m} + \Upsilon(m+1 \to m)u_{n,m+1} + \Upsilon(m-1 \to m)u_{n,m-1} \tag{10a}$$

$$0 = -\left(\frac{1}{T_2} + \frac{1}{t_n} + \frac{1}{s_n}\right)v_{n,m} + \gamma_e(H^0_{n,m} - H)u_{n,m} - \gamma_e H_{xy}\langle M_z\rangle_{n,m} + \Pi(n+1 \to n)v_{n+1,m} + \Pi(n-1 \to n)v_{n-1,m} + \Upsilon(m+1 \to m)v_{n,m+1} + \Upsilon(m-1 \to m)v_{n,m-1} \tag{10b}$$

where Π and Υ are the probabilities for spin density to rotate to an adjacent zone through angles β and γ, respectively, such that

$$\Pi(n+1 \to n) = \begin{cases} \dfrac{D_1}{\Delta_\beta^2}\dfrac{\sin(\beta_n + {}^1/_2\Delta_\beta)}{\sin(\beta_n + \Delta_\beta)} & 1 \le n \le N-1 \\ 0 & \text{otherwise} \end{cases} \tag{11a}$$

$$\Pi(n-1 \to n) = \begin{cases} \dfrac{D_1}{\Delta_\beta^2}\dfrac{\sin(\beta_n - {}^1/_2\Delta_\beta)}{\sin(\beta_n - \Delta_\beta)} & 2 \le n \le N \\ 0 & \text{otherwise} \end{cases} \tag{11b}$$

and

$$\Upsilon(m+1 \to m) = \Upsilon(m-1 \to m) = \frac{1}{\Delta_\gamma^2}\frac{D_1}{\sin^2\beta_n} + D_3 - D_1 \qquad 1 \le m \le M \text{ and } 1 \le n \le N \tag{11c}$$

The probabilities for spin density to rotate from adjacent zones into the (n,m)th zone for angles β and γ are

$$t_n \equiv \Pi(n \to n+1) + \Pi(n \to n-1) \tag{12a}$$

$$s_n \equiv \Upsilon(m \to m+1) + \Upsilon(m \to m-1) \tag{12b}$$

Finally, the time-averaged z component of the magnetization in the (n,m)th zone is

$$\langle M_z\rangle_{n,m} \propto \sin\beta_n \tag{13}$$

The appropriate spin Hamiltonian for application to the ^{15}N-substituted nitroxide spin labels is

$$H = \beta_e \mathbf{H}\cdot g\cdot\mathbf{S} + g_e\beta_e\mathbf{I}\cdot T\cdot\mathbf{S} \tag{14}$$

where β_e is the Bohr magneton, $\mathbf{H}$ is the Zeeman field vector, g is the g-tensor, $\mathbf{S}$ is the electron spin of the nitroxide radical, g_e is the g-factor of the free electron, $\mathbf{I}$ is the nuclear spin, and T is the T-tensor (Abragam & Bleany, 1970). Nuclear and electron spin magnitudes are both ${}^1/_2$. We compute the energy levels of the system to first order with bound state perturbation theory, treating the hyperfine term as a perturbation of the Zeeman term, and solve for the resonance Zeeman field $H^0_{n,m}$ (Merzbacher, 1970). We also calculate the spin transition probability and find that it is the same for each hyperfine line and mildly dependent on probe orientation.

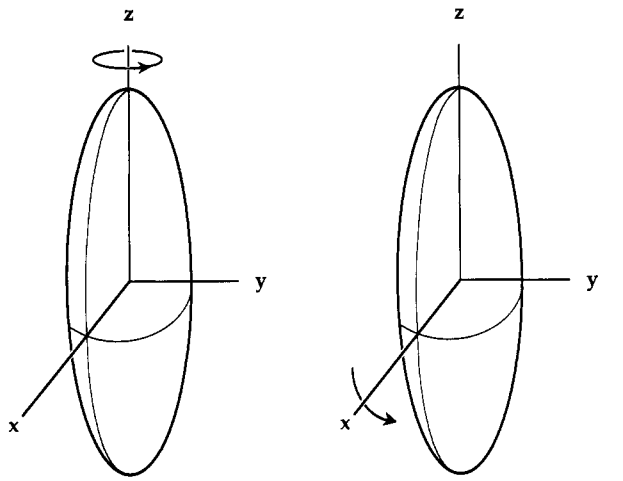

FIGURE 1: Principal hydrodynamic frame of a prolate ellipsoid of revolution showing the two degrees of rotational freedom. The ellipsoid has one fast axis (z), corresponding to torsional rotation (left), and two equivalent slow axes (x and y), corresponding to polar rotation (right). This model was chosen to approximate the shape of the isolated myosin S1.

It is assumed in eq 7 that the rotating frame is the principal hydrodynamic frame of the protein. The principal magnetic and hydrodynamic frames are generally not identical. Consequently, the resonant field in the principal hydrodynamic frame can contain off-diagonal elements of the g- and T-tensor coupling constants. We find that

$$H^0_{n,m}(m_I) = \frac{g_e}{(e^2_{n,m} + b_{n,m}b^*_{n,m})^{1/2}}\left(\frac{\hbar\omega}{\beta_e g_e} + m_I(c^2_{n,m} + 2d_{n,m}d^*_{n,m})^{1/2}\right) \tag{15}$$

where $2\pi\hbar$ is Planck's constant, $m_I = \pm{}^1/_2$ is the nuclear spin projection quantum number, and

$$e_{n,m} = -g_{x,z}\cos\gamma_m\sin\beta_n + g_{y,z}\sin\gamma_m\sin\beta_n + g_{z,z}\cos\beta_n \tag{16a}$$

$$b_{n,m} = (-g_{x,x} + ig_{x,y})\cos\gamma_m\sin\beta_n + (g_{x,y} - ig_{y,y})\sin\gamma_m\sin\beta_n + (g_{x,z} - ig_{y,z})\cos\beta_n \tag{16b}$$

$$c_{n,m} = (2e_{n,m}T_{z,z} + (b_{n,m} + b^*_{n,m})T_{x,z} + i(b_{n,m} - b^*_{n,m})T_{y,z})/(2(e_{n,m} + b_{n,m}b^*_{n,m})^{1/2}) \tag{16c}$$

$$d_{n,m} = ({}^1/_2)^{1/2}(2e_{n,m}(T_{x,z} - iT_{y,z}) + (b_{n,m} + b^*_{n,m})T_{x,x} + (b_{n,m} - b^*_{n,m})T_{y,y} - 2ib^*_{n,m}T_{x,y})/(2(e_{n,m} + b_{n,m}b^*_{n,m})^{1/2}) \tag{16d}$$

where $i = (-1)^{1/2}$.

The Euler rotation of the principal magnetic frame g-tensor elements, $g^p_{k,k}$, gives the off-diagonal tensor elements appearing in eq 16 such that

$$g_{i,j} = \sum_k E_{i,k}(\alpha_p,\beta_p,\gamma_p)\,E_{j,k}(\alpha_p,\beta_p,\gamma_p)\,g^p_{k,k} \tag{17}$$

where index $k = 1, 2, 3$, $E_{i,j}$ are elements of the Cartesian Euler rotation matrix, and Euler angles $(\alpha_p, \beta_p, \gamma_p)$ give the relationship between the principal magnetic frame and the principal hydrodynamic frame. A similar relationship holds for the T-tensor elements. Euler angles $(\alpha_p, \beta_p, \gamma_p)$ affect the shape of the EPR spectrum through eq 17 and the corresponding relationship for the T-tensor.

We solve for $v_{n,m}$ using the coupled eqs 10a and 10b with substitutions from eqs 11–17. The $v_{n,m}$'s, weighted by the transition probability, are summed over indices n and m to give the microwave absorption as a function of the Zeeman field.

(C.2) Effect of Independent Probe Movement on EPR. The independent movement of the spin label on the surface of the protein is an additional degree of freedom that may contribute to the shape of the EPR spectrum. Local probe rotational movement affects line shape by (i) causing the hyperfine split lines to have different widths (Nordio, 1976) and (ii) altering the resonant Zeeman field, $H^0_{n,m}$, because it depends on probe orientation. We include the effect of (i) by permitting each absorption line width to vary independently when searching for the spectral parameters of the best fit. We estimate the effect of (ii) by averaging $H^0_{n,m}$ over the domain of the local probe motion. This is dynamic averaging of $H_{m,n}$, and it is appropriate since the local probe movement is rapid relative to the time scale of spin–spin coupling relaxation or rotational relaxation due to protein motion.

We carry out the dynamic averaging of $H^0_{m,n}$ over a restricted domain corresponding to a single parameter, the cone angle, within which a probe fixed reference frame rotates. We account for the effect of local probe movement on the shape of steady-state EPR spectra from spin-labeled myosin S1 tumbling in solution or decorating actin in muscle fibers. We assume that spin-labeled S1 precipitated and immobilized in ammonium sulfate (the rigid limit sample) does not have local probe movement.

(C.3) Time-Resolved Fluorescence Anisotropy Decay (TRFAD). The TRFAD of fluorescent-labeled proteins in solution depends on the protein rotational diffusion constants and on the relationship of the principal hydrodynamic frame with the transition dipoles of the fluorescent probes. The TRFAD from freely diffusing and specifically labeled asymmetric proteins is a sum of five exponentials with amplitudes related to the orientation of the transition dipoles in the principal hydrodynamic frame and exponents related to the protein rotational diffusion constants (Favro, 1960; Ehrenberg & Rigler, 1972; Chuang & Eisenthal, 1972). Only one or two exponential decays are resolvable from TRFAD, giving insufficient information to specify the orientation of the transition dipoles in the principal hydrodynamic frame. We use TRFAD measurements to supplement data from multiple probes of the oriented sysem (combined by the multiple probe analysis) to obtain sufficient constraints to determine the dipole orientation within the protein principal hydrodynamic frame.

The independent movement of the fluorescent label on the surface of the protein is an additional degree of freedom that contributes to the TRFAD in a very simple way. When the probe moves rapidly relative to protein rotational relaxation, the two motions separate on the time domain so that the initial TRFAD is from the local probe movement. This initial decay is modeled by a single parameter giving the cone angle for the local probe movement (Lakowicz, 1983).

We use dynamic averaging of the probe transition dipole orientation to model the effect of local probe movement on the steady-state FP intensities from the fluorescent-labeled, oriented samples used in the multiple probe analysis. The averaging process accounts for local probe movement by altering the basis spectra $g_i^{FLS}(\psi,\chi,\lambda_{ex},\lambda_{em})$ from eq 3.

(D) Application to Problems in Muscle Contraction. We are interested in the angular distribution of the myosin S1 in the actin-bound physiological states of rigor, in the presence of the nucleotide MgADP, in isometric contraction, and in low ionic strength relaxed condition. The probes involved are the two spin labels, ^{15}N- and ^{2}H-substituted maleimido-TEMPO ([^{15}N,^{2}H]MTSL) and iodoacetamido-PROXYL ([^{15}N,^{2}H]IPSL), labeling sulfhydryl 1 (SH1) in myosin S1, and the two fluorescent labels 1,5-IAEDANS (1,5IA) and 5′-(iodoacetamido)tetramethylrhodamine (5-IATR), labeling SH1 on myosin cross-bridges in muscle fibers. The FP intensities of 1,5IA are measured at two excitation wavelengths.

Our past and present studies with fluorescent and spin labels were performed on two different but comparable biochemical systems. The fluorescent probes modify the cross-bridges in fibers without altering the ability of the muscle fiber to contract (Nihei et al., 1974; Crowder & Cooke, 1984). Because of the known problems in spin labeling intact fibers, we use spin probes to modify S1 and decorate unlabeled muscle fibers in rigor and in the presence of MgADP. The decorated fibers are the model system for the cross-bridge attached states in the contraction cycle. We investigate the active isometric and relaxed states directly with fluorescent-labeled fibers. The EPR and FP intensity data are sufficient to solve for the orientation of all investigated states of the cross-bridge.

If myosin S1 is a rigid body, then rotation of its principal hydrodynamic frame causes a similar rotation of all of the probe coordinate frames. This idea is the basis for the scheme indicated in Figure 2. If myosin is not a rigid body, then probes on different regions of S1 would rotate differentially. The multiple probe approach investigates both possibilities by telling whether or not the initial assumption of a rigid body rotation is consistent with the measured data.

(E) The Multiple Probe Analysis Program. Figure 2 shows the relationship among the probe and hydrodynamic reference frames. Each set of order parameters is numbered from 1 to 24 (as shown in parentheses in Figure 2) and corresponds to a particular probe and physiological state (e.g., set 1 determines the angular distribution of the MTSL probe in rigor). The relationship among the order parameter sets is completely described by eqs 4 and 5 and the three Euler angles represented by $\Omega_{i\rightarrow j}$. Observable quantities relate to the probe order parameters through eqs 2 and 3, and these in turn are relatable to all of the other order parameters through rotations of the forms in eqs 4 and 5. We set up our constraining equations by relating all observable quantities to order parameter set 9 (the principal hydrodynamic frame of a cross-bridge in a fiber in rigor), given explicitly by

$$\{a^j_{0,n}\} = \{a^0_{0,0}, a^1_{0,1}, a^1_{0,0}, a^1_{0,-1}, a^2_{0,2}, a^2_{0,1}, a^2_{0,0}, a^2_{0,-1}, a^2_{0,-2}, a^3_{0,3}, a^3_{0,2}, a^3_{0,1}, a^3_{0,0}, a^3_{0,-1}, a^3_{0,-2}, a^3_{0,-3}, a^4_{0,4}, a^4_{0,3}, a^4_{0,2}, a^4_{0,1}, a^4_{0,0}, a^4_{0,-1}, a^4_{0,-2}, a^4_{0,-3}, a^4_{0,-4}, a^6_{0,6}, a^6_{0,5}, a^6_{0,4}, a^6_{0,3}, a^6_{0,2}, a^6_{0,1}, a^6_{0,0}, a^6_{0,-1}, a^6_{0,-2}, a^6_{0,-3}, a^6_{0,-4}, a^6_{0,-5}, a^6_{0,-6}\} \quad (18)$$

and treat this set of 29 variables as unknowns. The best fitting solution for the unknowns is found by a linear least squares method (Strang, 1986). Solving for the rigor S1 hydrodynamic frame orientation (order parameter set 9) is a change from previous work made possible by independently solving for the Euler angles relating the probe orientation with the protein principal hydrodynamic frame. The independent information

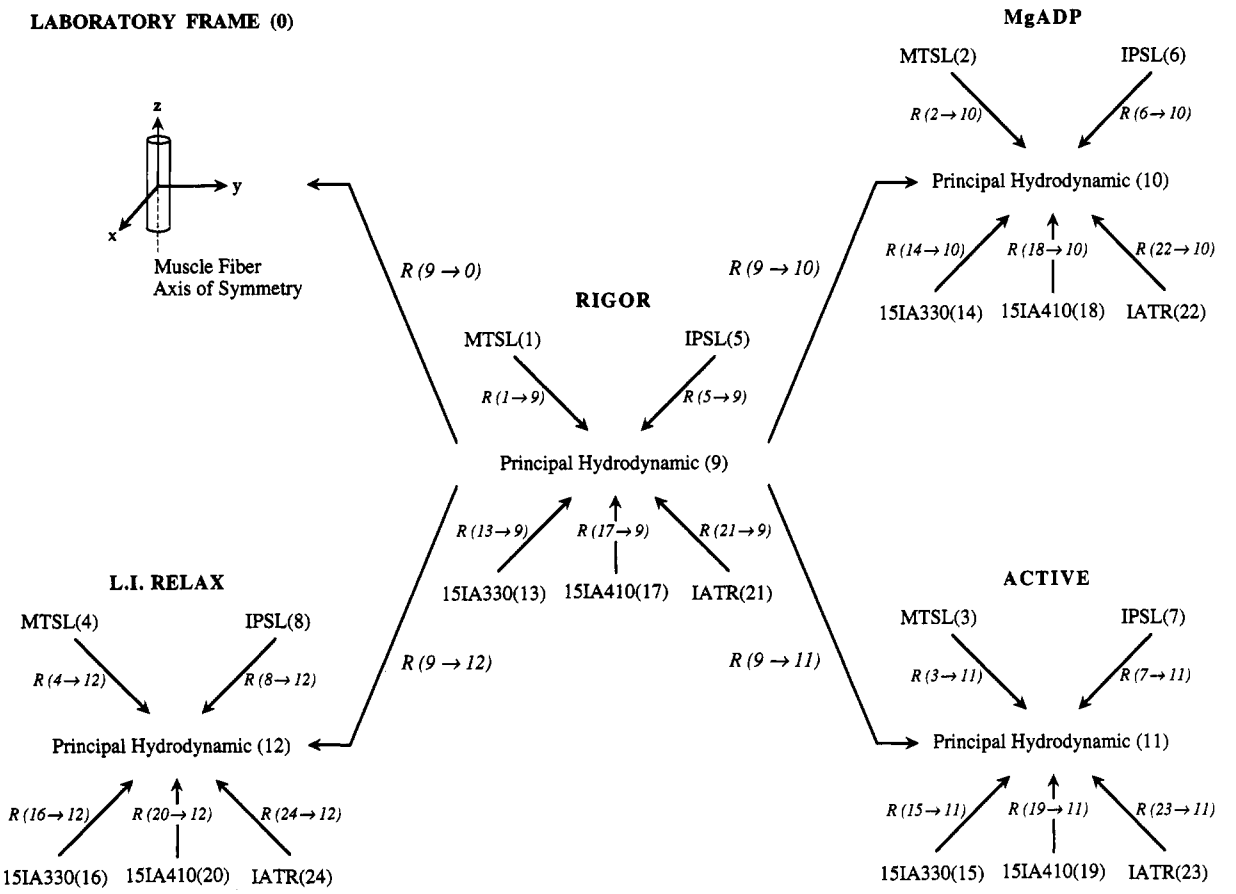

FIGURE 2: Relationship of reference frames in a multiprobe study of the myosin cross-bridge in muscle fibers. Each order parameter set is given a number from 1 to 24. Rotation matrices $R(i \rightarrow j)$ interrelate all of the sets of order parameters. The relationship between a probe and the protein principal hydrodynamic reference frame is independent of the protein physiological state [e.g., $R(1 \rightarrow 9)$ relates MTSL to the principal hydrodynamic frame of each physiological state such that $R(1 \rightarrow 9) = R(2 \rightarrow 10)$]. The relationship between any two hydrodynamic frames is independent of the probe fixed frame, but rotations relating the different protein states cause the similar rotation of all of the probe reference frames {e.g., $[R(1 \rightarrow 9)]^{-1} R(9 \rightarrow 10) R(1 \rightarrow 9)$ relates MTSL in rigor to MTSL in the MgADP state}. Rotation $R(9 \rightarrow 0)$ relates the most likely orientation of the rigor cross-bridge to the laboratory frame.

comes from the steady-state EPR measurements of spin-labeled S1 and time-resolved measurements of fluorescent-labeled S1, both freely diffusing in solution as described in part C of this section.

The set of unknown order parameters listed in eq 18 is larger than that used before since it includes odd-rank parameters where $j = 1$ and $j = 3$. We showed that the FP intensities of the oriented system measured from unusual combinations of the excitation and emission polarizers confer sensitivity of these signals to $j = 1$ and $j = 3$ order parameters. This is not the case when the FP intensities with ψ and χ, from eq 3, equal only 0 or 90° are the data set. We include FP intensities from all combinations of ψ and χ equal 0, 30°, 54.7°, or 90°.

Our present multiple probe investigation of cross-bridge orientation now includes two additional physiological states of muscle, that of active isometric contraction and that in low ionic strength relaxing conditions. The information from the fluorescent probes in these states broadens the data base, making the final solution more reliable and giving us insight into the path and extent of cross-bridge rotation in the active cycle. We accomplish a full solution of this problem without EPR data from active isometric or low ionic strength relaxed conditions.

DISCUSSION

It is certain that changes in cross-bridge orientation accompany changes in the physiological state of the muscle fiber. This is apparent from probe studies of cross-bridge orientation and order. However, further clarification of the path and extent of cross-bridge rotation during muscle contraction remains an important objective of muscle research. We begin work on this objective by fully describing how the principal hydrodynamic frame of S1 is oriented in different physiological states of the fiber and by investigating the intramolecular freedom of rotational movement in S1. To accomplish this we (i) developed methods to quantify protein orientation that are based on the analysis of data from multiple probes to increase the angular resolution of the estimated cross-bridge orientation distribution, (ii) focused our attention on the protein rather than the probe angular distribution by introducing independent data for estimating the relationship between the probe coordinate frame and the protein hydrodynamic frame, and (iii) used the multiple probe approach to ascertain whether the rigid body rotation of S1 reasonably accounts for the observed data. The result of this work is that we can estimate the cross-bridge angular distribution in four physiological states of the fiber, including isometric contraction, with higher angular resolution than was possible previously and with confidence that all of the probes are consistently telling the same story.

We showed how to increase the angular resolution of the observed angular distribution by including odd-rank order parameters in its description. This resolution enhancement increases the total number of order parameters found by experiment and removes a basic ambiguity in the way angular

distributions were described in the past. The odd-rank parameters break the reflection symmetry in the polar angular distribution at $\beta = 90°$ imposed by all EPR and the standard FP measurements of probe angular distributions. We are able to do this for all of the physiological states investigated.

We also showed how to focus the investigation of changes in cross-bridge orientation on the S1 principal hydrodynamic frame rather than on the probe frame of reference. This focus permits interpretation of the cross-bridge rotation in more basic terms related to the identifiable shape of the myosin head. By this method we discovered that the cross-bridge functions appear to be distributed between its angular degrees of freedom such that the force generation is a polar rotation while ATPase is predominantly a torsional rotation. We also find that the probe data from SH1 are consistent with the notion that the cross-bridge rotates as a rigid body (Ajtai et al., 1994).

The multiple probe analysis of protein rotation is a versatile and general approach for detecting protein orientation and order changes. The ability to combine data from different probes and complementary techniques gives the evident advantages over single probe methods including less ambiguity and higher resolution in finally solving for the angular distribution. There is another advantage of our method that we have made use of in our application to muscle fibers. The complementary techniques of EPR and FP are not equally suitable for each application. EPR has a lower signal-to-noise ratio than FP. This is evident from the sample size needed since a good EPR spectrum requires a bundle of labeled fibers and several minutes of collection time while FP can be done on $\sim$1-μm^3 volumes of single fibers with a time resolution of submilliseconds (Borejdo et al., 1979; Valez & Axelrod, 1988). On the other hand, EPR contains more information on the orientation distribution of the probe. Clearly FP is the only choice for investigating cross-bridge orientation from the active state since active fibers use up MgATP, and substrate diffusion in a bundle of fibers is well-known to be rather slow. EPR probes also have the specificity problems we have mentioned that prohibit their use in intact fibers. However, with the use of the multiple probe analysis the problems of applying EPR to isometric fibers are worked around without reducing the impact of the other advantages of EPR.

In the accompanying paper we demonstrate the applicability of our new methods to the investigation of the molecular mechanism of muscle contraction (Ajtai et al., 1994). There we study static states of the muscle fiber and deduce the angular distribution of the cross-bridge as a function of the fiber state. Because the static states of the fiber can be placed in chronological order, based on the apparent free energy liberated by the ATP hydrolysis available for force generation, we observe the path for cross-bridge rotation. The power of the method introduced here may be more fully realized in the near future when the good time resolution of FP polarization measurements is used to quantify cross-bridge movement. With the multiprobe analysis, time-resolved FP will investigate the protein rotational trajectory in real time.

REFERENCES

Abragam, A., & Bleany, B. (1970) *Electron Paramagnetic Resonance of Transition Ions*, pp 133–209, Dover, New York.

Ajtai, K., & Burghardt, T. P. (1986) *Biochemistry 25*, 6203–6205.

Ajtai, K., Ringler, A., & Burghardt, T. P. (1992) *Biochemistry 31*, 207–217.

Ajtai, K., Toft, D. J., & Burghardt, T. P. (1994) *Biochemistry* (following paper in this issue).

Belágyi, J. (1975) *Acta Biochim. Biophys. Acad. Sci. Hung. 10*, 233–242.

Borejdo, J., Putnam, S., & Morales, M. F. (1979) *Proc. Natl. Acad. Sci. U.S.A. 76*, 6346–6350.

Borejdo, J., Assulin, O., Ando, T., & Putnam, S. (1982) *J. Mol. Biol. 158*, 391–414.

Burghardt, T. P. (1984) *Biopolymers 23*, 2383–2406.

Burghardt, T. P., & Ajtai, K. (1990) in *Molecular Mechanisms in Muscular Contraction* (Squire, J., Ed.) pp 211–239, Macmillan, London.

Burghardt, T. P., & Ajtai, K. (1992) *Biochemistry 31*, 200–206.

Burghardt, T. P., Ando, T., & Borejdo, J. (1983) *Proc. Natl. Acad. Sci. U.S.A. 80*, 7515–7519.

Chuang, T. J., & Eisenthal, K. B. (1972) *J. Chem. Phys. 57*, 5094–5097.

Crowder, M. S., & Cooke, R. (1984) *J. Muscle Res. Cell Motil. 5*, 131–146.

Davydov, A. S. (1963) *Quantum Mechanics*, pp 145–169, NEO Press, Ann Arbor, MI.

Ehrenberg, M., & Rigler, R. (1972) *Chem. Phys. Lett. 14*, 539–544.

Favro, L. D. (1960) *Phys. Rev. 119*, 53–62.

Freed, J. H. (1976) in *Spin Labeling: Theory and Applications* (Berliner, L. J., Ed.) pp 53–132, Academic Press, New York.

Goldman, S. A., Bruno, G. V., Polnaszek, C. F., & Freed, J. H. (1972) *J. Chem. Phys. 56*, 716–735.

Lakowicz, J. R. (1983) *Principles of Fluorescence Spectroscopy*, pp 111–150, Plenum Press, New York.

McCalley, R. C., Shimshick, E. J., & McConnell, H. M. (1972) *Chem. Phys. Lett. 13*, 115–119.

Merzbacher, E. (1970) *Quantum Mechanics*, pp 413–450, John Wiley, New York.

Nihei, T., Mendelson, R. A., & Botts, J. (1974) *Biophys. J. 14*, 236–242.

Nordio, P. L. (1976) in *Spin Labeling: Theory and Applications* (Berliner, L. J., Ed.) pp 5–52, Academic Press, New York.

Strang, G. (1986) in *Introduction to Applied Mathematics*, pp 87–137, Wellesley-Cambridge Press, Wellesley, MA.

Thomas, D. D., & Cooke, R. (1980) *Biophys. J. 32*, 891–906.

Valez, M., & Axelrod, D. (1988) *Biophys. J. 53*, 575–591.